Submitted, accepted and published by:
Journal of Power Sources 192 (2009) 27–34

Hydrogen production by chemical-looping reforming in a circulating fluidized bed reactor using Ni-based oxygen carriers

Luis F. de Diego*, María Ortiz, Francisco García-Labiano, Juan Adánez, Alberto Abad, and Pilar Gayán

Department of Energy and Environment, Instituto de Carboquímica (C.S.I.C.)

Miguel Luesma Castán 4, 50018 Zaragoza, Spain

Phone number: +34 976 733 977

Fax number: +34 976 733 318

E-mail: ldediego@icb.csic.es

*Corresponding Author. Tel.: +34-976-733977; fax: +34-976-733318; E-mail address: ldediego@icb.csic.es (L.F. de Diego)[1]

Abstract

This work presents the experimental results obtained during auto-thermal chemical looping reforming (CLR) in a 900 W_{th} circulating fluidized bed reactor under continuous operation using methane as fuel. Two oxygen carriers based on NiO and supported on γ-Al_2O_3 and α-Al_2O_3 were used during more than 50 hours of operation with each oxygen carrier. During operation the effect of different operating variables,

[1] Presented at CONAPPICE 2008, Zaragoza, Spain, 24-26 September 2008

like fuel reactor temperature, H_2O/CH_4 molar ratio and solid circulation rate, on CH_4 conversion and gas product distribution was analyzed. It was found that in all operating conditions CH_4 conversion was very high (>98%) and the most important variable affecting to the gas product distribution was the solid circulation rate, that is, NiO/CH_4 molar ratio. Similar gas product distribution was obtained working with both oxygen carriers although at different NiO/CH_4 molar ratios. The oxygen carrier of NiO on α-Al_2O_3 needed lower NiO/CH_4 molar ratio to reach the same gas product composition than the oxygen carrier of NiO on γ-Al_2O_3. Working at optimal operating conditions, 2.5 moles of H_2 per mol of CH_4 could be obtained in this process.

During operation the oxygen carrier particles maintained their physical and chemical properties. These results suggest that these oxygen carriers could have a high durability, being suitable oxygen carriers for a CLR system.

Keywords: Hydrogen, Chemical looping, Oxygen carrier, Nickel oxide, Fluidized bed

1. Introduction

It is widely accepted today that carbon dioxide coming from fossil fuel combustion is the most important greenhouse gas contributing to global warming. One of the options to overcome anthropogenic greenhouse effect is the development of CO_2 capture and storage technologies from flue gases of power plants. However, CO_2 capture technology applied to transport sector is more complex, being the use of H_2 as fuel one possible option to reduce the CO_2 emissions.

Steam reforming of CH_4 is the most widely used technology for H_2 production, although, this method produces also large amounts of CO_2 as by-product. CO_2 capture technology integrated with H_2 production is available today being high cost the main barrier to its use. In the CACHET project the integration of CO_2 capture technologies with H_2 production systems for power generation and fuel applications are being studied [1]. The overall goal of the CACHET project is to develop innovative technologies which will substantially reduce the cost of CO_2 capture whilst simultaneously producing H_2 from natural gas fuel. Some of the technologies investigated are based in Chemical-Looping Combustion (CLC) process.

CLC is a novel combustion technology with inherent separation of the greenhouse gas CO_2 that involves the use of an oxygen carrier, which transfers oxygen from air to the fuel avoiding the direct contact between them. CLC system is made of two interconnected reactors, designated as air and fuel reactors. In the fuel reactor, the fuel gas (C_nH_{2m}) is oxidized to CO_2 and H_2O by a metal oxide (MeO) that is reduced to a metal (Me) or a reduced form of MeO. The metal or reduced oxide is further transferred into the air reactor where it is oxidized with air, and the material regenerated is ready to start a new cycle. The flue gas leaving the air reactor contains N_2 and unreacted O_2. The exit gas from the fuel reactor contains only CO_2 and H_2O. After water condensation, almost pure CO_2 can be obtained with little energy lost for component separation.

Chemical-Looping auto-thermal Reforming (CLR) also uses the metal oxide to transfer oxygen to the fuel, being the main difference that the desired product is syngas (H_2 + CO). In the CLR process the air to fuel ratio is kept low to prevent the complete

oxidation of the fuel to CO_2 and H_2O. The major advantage of this process is that the heat needed for converting CH_4 to H_2 is supplied without costly oxygen production, without mixing of air with carbon containing fuel gases or without using part of the H_2 produced in the process. An important aspect to be considered in a CLR system is the heat balance. The oxidation reaction of the metal oxide is very exothermic, however, the reduction reactions are endothermic. So, the heat for the endothermic reduction reactions is given by the circulating solids coming from the air reactor at higher temperature. The heat generated in the air reactor must be enough high to fulfil the heat balance in the system.

CLR, as described in Figure 1, was proposed by Mattisson et al. [2]. These authors [3] examined the thermodynamics and the heat balance of the fuel and air reactors using CuO/SiO_2 and NiO/SiO_2 as oxygen carriers and found that, in order to maintain a high temperature and CH_4 conversion, the fraction of oxygen supplied by the steam should not exceed approximately 0.3 of the total oxygen added to the fuel reactor. In addition, they found that the selectivity towards H_2 production was higher with the NiO/SiO_2 oxygen carrier than with the CuO/SiO_2 oxygen carrier.

An oxygen carrier for CLR should have the following properties: enough reactivity through cycles to reduce solids inventory; high resistance to attrition to minimize losses of elutriated solid; complete fuel conversion to CO and H_2; negligible carbon deposition what would release CO_2 in the air reactor and good properties for fluidization (no presence of agglomeration). In addition, other characteristics such as easy preparation to reduce costs are interesting. Iron, nickel, copper and manganese are promising active

metals to be used in a CLR process, but Ni appears the most interesting due to its strong catalytic properties. Metallic Ni is used in most commercial steam reforming catalyst.

There are some works studying different oxygen carriers for CLR. Zafar et al. [4-5] tested in a laboratory fluidized bed reactor and in a thermogravimetric analyzer (TGA) different oxygen carriers consisting of oxides of Fe, Mn, Ni and Cu supported on SiO_2 and $MgAl_2O_4$. They observed that working at 950 ºC, the oxygen carriers based on Ni, Fe, and Mn and supported on SiO_2 underwent considerable reactivity deactivation with the redox cycles. On the contrary all of the $MgAl_2O_4$-supported oxygen carriers showed high reactivities during reduction and oxidation, and the Ni-based carriers showed the highest selectivity toward H_2.

Several oxygen carriers for CLR have been also tested by Ryden et al [6] in a fixed bed reactor. They found that $La_xSr_{1-x}FeO_{3-\delta}$ perovskites provided very high selectivity towards CO/H_2. $Fe_2O_3/MgAl_2O_4$ with or without added $NiO/MgAl_2O_3$ was found to have properties that could be useful for CLR, and $Mn_3O_4/Mg\text{-}ZrO_2$ with or without added $NiO/MgAl_2O_3$ was found to be suitable only for CLC. These authors [7] also worked in a continuous laboratory reactor consisting of two interconnected fluidized beds with an oxygen carrier made of NiO and $MgAl_2O_4$. Complete conversion of natural gas and high selectivity towards H_2 and CO was achieved. Formation of solid carbon was reduced or eliminated by adding steam to natural gas. These authors confirmed that the concept chemical-looping reforming is feasible and should be further investigated.

Johansson et al [8] compared two different oxygen-carriers, $NiO/NiAl_2O_3$ and $NiO/MgAl_2O_4$, using both continuous and pulse experiments in a batch laboratory fluidized bed. They found that $NiO/MgAl_2O_4$ offers higher methane conversion, higher selectivity to reforming and lesser tendency for carbon formation.

In a previous work, our group [9] studied in a TGA and in a batch fluidized bed reactor several Ni-based oxygen carriers prepared by impregnation on alumina. The tests carried out showed that Ni-based oxygen carriers prepared by incipient wetness impregnation on γ-Al_2O_3, θ-Al_2O_3, and α-Al_2O_3 are suitable for auto-thermal reforming of methane during long periods of time without carbon formation.

In this work, two selected Ni-based oxygen carriers, of the previously tested in the batch fluidized bed, have been used in a 900 W_{th} CLR continuous pilot plant to set the suitability of those materials for CLR. The effect of operating conditions, such as oxygen carrier-to-fuel ratio, fuel reactor temperature and the H_2O/CH_4 molar ratio, on the process efficiency has been analyzed.

2. Experimental Section

2.1. Materials

The behaviour of two oxygen carriers based on nickel was analyzed in this work. In both of them, Al_2O_3 was selected as support to increase the mechanical strength of the material. NiO21-γAl_2O_3 was prepared by incipient wetness impregnation over

Commercial γ-Al_2O_3 (Puralox NWa-155, Sasol Germany GmbH) and NiO18-αAl_2O_3 was prepared by incipient wetness impregnation over α-Al_2O_3 (obtained by calcination of γ-Al_2O_3 at 1150 ºC during 2 hours). The details of the preparation of both oxygen carriers have been described elsewhere [9-10]. The oxygen carriers are designated with the metal oxide followed by its weight content and the inert used as support.

2.2. Oxygen carrier characterization

The oxygen carriers were physically and chemically characterized by several techniques. The bulk density of the oxygen carrier particles was calculated weighting a known volume of solid and assuming that the void was 0.45 corresponding to loosely packed bed. The force needed to fracture a particle was determined using a Shimpo FGN-5X crushing strength apparatus. The mechanical strength was taken as the average value of at least 20 measurements. The porosity was measured by Hg intrusion in a Quantachrome PoreMaster 33. The identification of crystalline chemical species was carried out by powder X-ray diffraction (XRD) patterns acquired in an X-ray diffractometer Bruker AXS D8ADVANCE using Ni-filtered Cu Kα radiation equipped with a graphite monochromator. The oxygen carriers were also analyzed in a scanning electron microscope (SEM) ISI DS-130 coupled to an ultra thin window PGT Prism detector for energy-dispersive X-ray (EDX) analysis.

2.3. Reactivity tests in TGA

Reactivity tests of the oxygen carriers were carried out in a TGA, CI Electronics type, described elsewhere [11-12]. For the experiments, the oxygen carrier was loaded in a platinum basket and heated to the set operating temperature in air atmosphere. After weight stabilization, the experiment was started by exposing the oxygen carrier to alternating reducing and oxidizing conditions. The reducing gas was saturated in water by bubbling it through a water containing saturator at the selected temperature to reach the desired water concentration. The gas selected for the reducing experiments was composed by 15 vol.% CH_4, and 20 vol.% H_2O (N_2 balance) and the gas used for oxidation was 100 vol.% air. To avoid mixing of combustible gas and air, nitrogen was introduced for 2 min after each reducing and oxidizing period. The experiments were usually carried out at 950 ºC.

2.4. 900 W_{th} Experimental Facility

Figure 2 shows the schematic diagram of the 900 W_{th} continuous atmospheric CLR pilot plant used for the tests. The pilot plant was basically composed of two interconnected fluidized-bed reactors, a riser for solids transport from the air reactor (AR) to the fuel reactor (FR), a solid valve to control the flow rate of solids fed to the fuel reactor, a loop seal and a cyclone. This design allowed the variation and control of the solid circulation flow rate between both reactors.

The FR (1) consisted of a bubbling fluidized bed (0.052 m i.d.) with a bed height of 0.1 m. In this reactor the NiO of the oxygen carrier is reduced by the fuel to Ni. Reduced oxygen carrier particles overflowed into the AR (3) through a U-shaped fluidized bed

loop seal (2), to avoid gas mixing between fuel and air. The oxidation of the carrier took place at the AR, which consisted of a bubbling fluidized bed (0.05 m i.d.) with a bed height of 0.1 m, followed by a riser (4) of 0.02 m i.d. and 1 m height. The regeneration of the oxygen carrier happened in the dense bed part of the AR allowing residence times high enough for the complete oxidation of the reduced carrier. Secondary air could be introduced at the top of the bubbling bed to help particle entrainment. N_2 and unreacted O_2 left the AR passing through a high-efficiency cyclone (5) and a filter (9) before the stack. The oxidized solid particles recovered by the cyclone were sent to a solids reservoir setting the oxygen carrier ready to start a new cycle. In addition, these particles avoid the leakage of gas between the FR and the riser. The regenerated oxygen carrier particles returned to the FR by gravity from the solids reservoir through a solids valve (7) which controlled the flow rates of solids entering the FR. A diverting solids valve (6) located below the cyclone allowed the measurement of the solids flow rates at any time. Fine particles produced by fragmentation/attrition in the plant were recovered in the filters that were placed downstream of the FR and AR.

The prototype had several tools of measurement and system control. Thermocouples and pressure drop transducers located at different points of the plant showed the current operating conditions in the plant at any time. Specific mass flow controllers gave accurate flow rates of feeding gases and H_2O. The gas outlet streams of the FR and AR were drawn to respective on-line gas analyzers to get continuous data of the gas composition. CH_4, CO, CO_2, and H_2O were measured at the fuel reactor outlet by two infrared gas analyzers, via Fourier transform infrared (FTIR, Temet CX4000) and nondispersive infrared (NDIR, Maihak S710/OXOR-P) analyses. H_2 was measured

using a thermal conductivity analyzer (Maihak S710/THERMOR). At the outlet of air reactor, CO and CO_2 were measured by an NDIR analyzer (Siemens/Ultramat 22P), and O_2 by a paramagnetic analyzer (Siemens/Oxymat 5E). All data were collected by means of a data logger connected to a computer.

After construction of the prototype, initial tests of solids circulation were carried out with air to learn about the control of the plant. In addition, gas leakage between the reactors was examined. It was fed a known flow of CO_2 tracer together with the fluidization gas in the fuel reactor, air reactor and loop seal and its concentration was measured at the outlet of the fuel and air reactors. This allowed us to know the gas distribution between the two branches in the loop seal at different operating conditions. The flow of N_2 introduced in the loop seal produces a dilution in the gas streams obtained at the outlet of the fuel and air reactors, and it was considered to correct the gas concentrations measured in the analyzers and for mass balance calculations. No mixing of gases of the fuel and air reactors and a similar gas distribution between the two branches of the loop seal was observed in the majority of the operating conditions.

3. Results and discussion.

Reforming tests under different operation conditions were conducted in the facility with the two oxygen carriers using CH_4 as fuel. The total solids inventory in the system was about 1.5 kg of solid material for both oxygen carriers. The selected range of operating conditions (with the exception of the solid circulation rate) was the same for the two oxygen carriers. To study the effect of the reduction temperature on the CH_4 conversion,

the temperature in the FR was varied over a range of 800-900 ºC. The temperature in the AR was always kept constant at about 950±15 ºC. The gas fed to the FR was composed of 50 vol.% of CH_4 and 50 vol.% of H_2O+N_2. The H_2O/CH_4 molar ratio was varied in the feeding gas from 0 to 0.5, so the composition of the feeding gas was 50 vol.% CH_4, 0-25 vol.% H_2O, and balanced N_2. The inlet flow of methane was 87.2 Nl h^{-1}, it means that the inlet gas velocity in the fuel reactor was 10 cm s^{-1} at 900 ºC. The inlet air flow in the AR was 720 Nl h^{-1} as primary air and 150 Nl h^{-1} as secondary air. The effect of oxygen carrier to fuel ratio on the methane conversion and gas product distribution was analyzed by controlling the solid circulation flow rates by means of the solids valve, and took values from 1 to 11 kg h^{-1}.

The steady-state for the different operating conditions was maintained at least for an hour in each test. A total of more than 50 hours of operation with each oxygen carrier, from which more than 40 h corresponded to the reaction period, were carried out.

3.1. Evaluation of the data

The gases product concentrations of the fuel and air reactors were measured by on line analyzers. These gases concentrations were recalculated taking into account the N_2 dilution coming from the loop seal, and were used to make carbon, hydrogen and oxygen mass balances over the whole reactor system, to verify that it was working properly.

The main reactions happening with different contribution in the fuel reactor during the oxygen carrier reduction period are:

Oxidation

$CH_4 + 4\ NiO \leftrightarrow 4\ Ni + CO_2 + 2\ H_2O$ (R1)

$H_2 + NiO \leftrightarrow Ni + H_2O$ (R2)

$CO + NiO \leftrightarrow Ni + CO_2$ (R3)

Partial oxidation

$CH_4 + NiO \leftrightarrow Ni + CO + 2\ H_2$ (R4)

Steam reforming catalyzed by Ni

$CH_4 + H_2O \leftrightarrow CO + 3\ H_2$ (R5)

Methane decomposition catalyzed by Ni

$CH_4 \leftrightarrow C + 2\ H_2$ (R6)

Carbon gasification

$C + H_2O \leftrightarrow CO + H_2$ (R7)

$C + CO_2 \leftrightarrow 2\ CO$

(R8)

Water gas shift

$CO + H_2O \leftrightarrow CO_2 + H_2$ (R9)

And in the air reactor during the oxygen carrier oxidation:

$Ni + ½\ O_2 \leftrightarrow NiO$ (R10)

$C + O_2 \leftrightarrow CO_2$ (R11)

$C + 1/2O_2 \leftrightarrow CO$ (R12)

Taking into account these reactions, the conversions of the oxygen carriers during the reduction and oxidation periods were calculated from the gas outlet concentrations by the equations:

Reduction

$$X_{red} = \frac{Q_{out}}{n_0\ P_{tot}}\left(2P_{CO_2,out} + P_{CO,out} + P_{H_2O,out}\right) \quad (1)$$

$$Q_{out} = Q_{in}\left(\frac{P_{N_2 in}}{P_{N_2 out}}\right) = Q_{in}\left(\frac{P_{N_2,in}}{(1 - P_{CH_4,out} - P_{CO_2,out} - P_{CO,out} - P_{H_2,out} - P_{H_2O,out})}\right) \quad (2)$$

Oxidation

$$X_{oxi} = \frac{2\,Q_{out}}{n_0\ P_{tot}}\left(\frac{Q_{in}}{Q_{out}}P_{O_2,in} - P_{O_2,out} - 1/2P_{CO,out} - P_{CO_2,out}\right) \quad (3)$$

$$Q_{out} = \frac{Q_{in}(1 - P_{O_2,in})}{(1 - P_{CO_2,out} - P_{CO,out} - P_{O_2,out})} \quad (4)$$

where X is the conversion of the oxygen carrier, Q_{in} is the molar flow of the gas coming into the reactor, Q_{out} is the molar flow of the gas leaving the reactor, P_{tot} is the total pressure, $P_{i,in}$ is the partial pressure of gas i coming into the reactor, $P_{i,out}$ is the partial pressure of gas i exiting the reactor, n_0 are the moles of oxygen which can be removed from fully oxidized oxygen carrier. The last terms in equation 3 take into account the formation of CO and CO_2 during the oxidation period due to the oxidation of C (reactions R11 and R12) coming from the decomposition of CH_4 (reaction R6) in the fuel reactor.

For better comparison, the results showed in this work are presented in N_2 free basis and/or dry N_2 free basis.

3.2. Effect of Fuel Reactor Temperature

The effect of fuel reactor temperature was tested in the range of 800-900ºC. Under all operating conditions, the inlet molar flow of methane was maintained constant. Figures 3 and 4 show the effect of fuel reactor temperature on the gas product concentrations for both oxygen carriers. It can be observed that the CH_4 conversion was very high (>98%) in all range of temperature tested. It can be also seen that for the same oxygen carrier-to-fuel ratio, an increase in the fuel reactor temperature produced a small increase in the CH_4 conversion, a slight increase in the CO_2 and H_2O concentrations and a slight decrease in the H_2 and CO concentrations for both oxygen carriers. The increase in the CH_4 conversion with increasing the FR temperature could be due to the increase of R1, R4, and R5 reaction rates, and the increase in the CO_2 and H_2O concentrations and

decrease in the H_2 and CO concentrations due to the increase of R1, R2, and R3 reaction rates. It must be taken into account that an increase in the FR temperature increased the reduction degree (that is the conversion) of the oxygen carrier and as a consequence more oxygen was available for oxidation of CH_4, H_2, and CO.

3.3. Effect of H_2O/CH_4 molar ratio

The H_2O/CH_4 molar ratio was varied from 0 to 0.5 (0 – 25% H_2O) in the fuel gas fed to FR. Figures 5 and 6 show the effect of H_2O/CH_4 molar ratio on the gas product concentration at the exit of the FR with different oxygen carrier-to-fuel ratios. An increase in H_2O/CH_4 molar ratio produced a slight increase of H_2 and CO_2 concentrations and a slight decrease of CO concentration, because H_2O enhances the methane reforming reaction (reaction R5) and specially the water gas shift reaction (reaction R9). Very similar results were found with both carriers.

In these tests, working without feeding H_2O (H_2O/CH_4 = 0) and with low solid circulation rates (e.i. low NiO/CH_4 molar ratios), CO and/or CO_2 were detected at the outlet of the AR due to the reactions R11 and R12. This indicated carbon formation due to reaction R6. Thermodynamic analyses show that in order to reach carbon free operation working with Ni-based oxygen carriers the O/C molar ratio must be higher than 1, being $O/C=(O_{H2O}/C)+(O_{NiO}/C)$, where: O_{H2O}= oxygen coming from the H_2O and O_{NiO}= oxygen coming from the oxygen carrier. The O_{NiO}/C molar ratio depends on different factors, the most important being the oxygen carrier reactivity and the NiO content in the carrier. So, for a given temperature, solid circulation rate, and oxygen

carrier (O_{NiO}/C=constant), an increase in the O_{H2O}/C molar ratio increases the O/C molar ratio and decrease the carbon formation.

3.4. Effect of Oxygen Carrier-to-Fuel Ratio

A basic operating parameter for CLR process is the oxygen carrier-to-fuel molar ratio which, for a given fuel flow rate fed to the FR, depends on the solid circulation flow rate between both reactors. In the pilot plant the solid circulation flow rates were controlled by means of the solids valve, and took values from 1 to 11 kg h^{-1}.

Figures 5 and 6 show the effect of oxygen carrier-to-fuel ratio (expressed as ratio between the moles of NiO loaded in the sample and the CH_4 moles fed into the FR) on the gas product concentration measured at the outlet of the FR for both oxygen carriers working with different H_2O/CH_4 molar ratios at a temperature of 900 ºC. It can be observed that the achieved methane conversion was very high and how an increase in the oxygen carrier-to-fuel ratio produced an increase in the CO_2 and H_2O concentrations and a decrease in the H_2, CO and CH_4 concentrations. This was obviously due to the different contribution of the different reactions (R1 to R9) to the overall global process, but specially increasing the oxygen carrier circulation flow rate increased the contribution of the oxidation reactions (reactions R1-R3).

Analyzing the measured gas product distributions, it was observed that similar gas product compositions were obtained with both oxygen carriers although working with different values of the NiO/CH_4 molar ratio. The NiO18-αAl_2O_3 oxygen carrier needed

lower oxygen carrier-to-fuel ratios than the NiO21-γAl_2O_3 oxygen carrier to obtain almost the same gas product composition. This effect was due to the difference in the reduction reactivity of both oxygen carriers, as can be inferred from Figure 7. This Figure shows the reactivity measured in the TGA for both oxygen carriers using as reacting gases 15 vol.% CH_4 and 20 vol.% H_2O (N_2 balance) for the reduction and pure air for the oxidation. As it can be seen, both oxygen carriers exhibited very high reactivity during oxidation, however, the NiO18-αAl_2O_3 oxygen carrier showed higher reactivity than the NiO21-γAl_2O_3 oxygen carrier during the reduction reaction. It seems that the low reduction reactivity of the carrier of NiO on γ-Al_2O_3 was due to the solid state reaction between the NiO and the γ-Al_2O_3 to form $NiAl_2O_4$, as it is shown in the XRD patterns (see Table 1). It must be taken into account that the reaction rate of CH_4 with $NiAl_2O_4$ is lower than with free NiO [9]. On the contrary, the high reactivity of the carrier of NiO on α-Al_2O_3 was because the interaction between the NiO and the support was reduced using the α-Al_2O_3. As can be seen in Table 1, free NiO was observed in this oxygen carrier. The presence of an important fraction of active NiO was also visually confirmed because the oxygen carriers prepared with α-Al_2O_3 were green coloured against blue samples containing high fractions of $NiAl_2O_4$, as it was the case of the carriers prepared with γ-Al_2O_3.

Figure 8 shows the conversions reached by the two oxygen carriers, calculated with equations (1) to (4), working at 900ºC and H_2O/CH_4=0.3. It was found that for similar operating conditions the conversions reached by the oxygen carrier with higher reactivity, NiO18-αAl_2O_3, were higher than the conversions reached by the oxygen carrier with lower reactivity, NiO21-γAl_2O_3. In addition, it can be seen that, mainly

working with the NiO21-γAl_2O_3 oxygen carrier, increasing the oxygen carrier-to-fuel ratio decreased the oxygen carrier conversion because, for the same oxygen carrier inventory in the reactor, an increase in the oxygen carrier-to-fuel ratio, that is in the oxygen carrier circulation rate, produced a decrease in the mean residence time of the oxygen carrier in the FR.

Taking into account the conversions reached by the oxygen carriers, Figure 9 shows the gas product composition measured at the outlet of the FR, working at 900 ºC with different H_2O/CH_4 molar ratios, as a function of the reacted NiO to CH_4 molar ratio for both oxygen carriers. It can be observed very similar gas composition at the outlet of the fuel reactor working with both oxygen carriers when the reacted NiO to CH_4 molar ratio was the same, and, in addition, it was found that these gas product compositions were close to thermodynamic equilibrium. Finally, it can be also seen in this figure that the best gas composition in order to maximize the H_2 production was obtained at low reacted NiO to CH_4 molar ratios ($NiO_{reacted}/CH_4 \approx 1$).

As mentioned above, an important aspect to be considered in a CLR system is the heat balance. The oxidation reaction of the metal oxide is very exothermic, however, the reduction reactions are endothermic. So, the heat necessary for the endothermic reduction reactions is given by the hot solids coming from the air reactor. The heat generated in the air reactor must be high enough to fulfil the heat balance in the whole system. A $NiO_{reacted}/CH_4$ molar ratio of ≈1.25 was calculated to the fulfilment of the heat balance. In these operating conditions a dry gas product composition of ≈65vol.% H_2, ≈25vol.% CO, ≈9 vol.% CO_2, and ≈1-1.5 vol.% CH_4 can be obtained in the auto-

thermal CLR process working with both carriers. This composition corresponds to 1.8 moles of H_2, 0.7–0.75 moles of CO and 0.25–0.3 moles of CO_2 per mol of CH_4 fed to the reactor. It means that, after water gas shift reactor, 2.5 moles of H_2 per mol of CH_4 can be obtained in this process.

3.5. Behaviour of the oxygen-carrier particles

A total of more than 50 hours of operation with each oxygen carrier, from which more than 40 hours corresponded to the reaction period, were carried out. The oxygen carrier particles never showed agglomeration or defluidization problems and the loss of fine solids due to attrition was negligible.

Figure 7 shows the reactivities measured in the TGA for the fresh and used oxygen carriers. The reduction and oxidation reactivities of the NiO18-αAl_2O_3 oxygen carrier were not affected by the operation, however, the reduction reactivity of the NiO21-γAl_2O_3 oxygen carrier was higher in the used particles. Table 1 shows the main properties of the oxygen carriers both fresh and after ≈50 hours of operation. The density of the used particles did not change for the NiO18-αAl_2O_3 oxygen carrier and a small increase was found for the NiO21-γAl_2O_3. A slightly decreased of the mechanical strength of the particles for both oxygen carriers was observed. The carrier porosity slightly decreased for both oxygen carriers with the respective mean pore size shifting towards pores of higher size, as shown in Figure 10. The BET specific surface area decreased for both carriers, and this effect was very noticeable in the carrier prepared on γ-Al_2O_3. These features suggest that some accumulative thermal sintering was occurring

in the oxygen carrier particles along the time during operation in the prototype but, fortunately, they did not deactivate the carrier reactivity, as shown in Figure 7. The powder XRD patterns of the used carrier NiO18-αAl_2O_3 revealed no new crystalline phases, however, the XRD patterns of the used NiO21-γAl_2O_3 revealed the presence of a new crystalline phase, NiO, and they also revealed that after 50 hours of operation γ-Al_2O_3 did not evolved to α-Al_2O_3.

The oxygen carrier particles were also analyzed by SEM-EDX. Figure 11 shows images of particles of the NiO21-γAl_2O_3 oxygen carrier, fresh and after operation. As shown in Figure 11a and b, the oxygen carrier particles exhibited an irregular shape and the general appearance of the used particles was similar to the fresh particles. No changes in the surface texture and the solid structure of the used particles were detected, compared to fresh particles.

The nickel distribution inside the particles was analyzed by EDX in some particles embedded in resin epoxy, cut, and polished. In both oxygen carriers, the Ni was uniformly distributed through the particles and there was not evidence of redistribution or migration of Ni sites during the redox cycles. These results suggest that these oxygen carriers could have a high durability, being suitable oxygen carriers for a CLR system.

4. Conclusions

Two Ni-based oxygen carriers, NiO21-γAl_2O_3 and NiO18-αAl_2O_3, prepared by incipient wetness impregnation, have been tested in a 900 W_{th} CLR pilot plant to analyze their

behaviour with regarding to the reforming of CH_4. During operation the effect of different operating variables, like fuel reactor temperature, H_2O/CH_4 molar ratio and solid circulation rate, on CH_4 conversion and gas product distribution was analyzed.

It was observed that in all operating conditions, with both oxygen carriers, the CH_4 conversion was very high (>98%). An increase in the reduction reaction temperature produced a slight increase in the CH_4 conversion and CO_2 and H_2O concentrations and a slight decrease in the H_2 and CO concentrations. An increase in H_2O/CH_4 molar ratio produced a small increase in the CO_2 and H_2 concentrations and a small decrease in the CO concentration. The most important operating variable affecting the gas product distribution was the oxygen carrier circulation rate, that is, the NiO/CH_4 molar ratio. An increase in the NiO/CH_4 molar ratio produced an increase in the CO_2 and H_2O concentrations and a decrease in the H_2, CO and CH_4 concentrations.

Similar gas product compositions were obtained with both oxygen carriers although working with different oxygen carrier circulation rate. The NiO18-αAl_2O_3 oxygen carrier, due to its higher reactivity, needed lower solid circulation rate than the NiO21-γAl_2O_3 oxygen carrier to obtain almost the same gas product composition.

The best gas product composition was obtained for $NiO_{reacted}/CH_4$ molar ratios near 1. However, a $NiO_{reacted}/CH_4$ molar ratio of ≈1.25 was calculated to the fulfillment of the heat balance. In these operating conditions a dry gas product composition of ≈65vol.% H_2, ≈25vol.% CO, ≈9 vol.% CO_2, and ≈1-1.5 vol.% CH_4 can be obtained in the auto-

thermal CLR process working with both carriers. In this way, after water gas shift reactor, 2.5 moles of H_2 per mol of CH_4 can be obtained in this process.

Important changes in the reactivity, surface texture and the solid structure of the oxygen carrier particles were not detected after 50 hours of operation. In addition, the oxygen carriers did not show agglomeration or defluidization problems and the loss of fine solids due to attrition was negligible. These results suggest that these oxygen carriers could have a high durability, being suitable oxygen carriers for a CLR system.

Acknowledgments

This work was partially supported by the European Commission, under the 6th Framework Programme (CACHET Project, Contract no. 019972), and from the CCP2 (CO_2 Capture Project), a partnership of BP, Chevron, Conoco-Phillips, Eni Technology, Norsk Hydro, Shell, Suncor, and Petrobras. M. Ortiz thanks Diputación General de Aragon for the F.P.I. fellowship.

References

[1] Carbon Dioxide Capture and Hydrogen Production from Gaseous Fuels (CACHET project). FP6-019972.

[2] T. Mattison, A. Lyngfelt. Proceedings of the 2nd Nordic Minisymposium on Carbon Dioxide Capture and Storage, Göteborg, Sweden, 2001.

[3] T. Mattison, Q. Zafar, A. Lyngfelt, B. Gevert. 15th World Hydrogen Energy Conference, Yokohama, Japan, 2004.

[4] Q. Zafar, T. Mattison , B. Gevert. Ind. Eng. Chem. Res., 44 (2005) 3485-3498.

[5] Q. Zafar, T. Mattison, B. Gevert. Energy Fuels, 20 (2006) 34-44.

[6] M. Ryden, A. Lyngfelt, T. Mattisson, D. Chen, A. Holmen, E. Bjørgum. Int. J. Greenhouse Gas Control, 2 (2008) 21-36.

[7] M. Ryden, A. Lyngfelt, T. Mattison. Fuel, 85 (2006) 1631-1641.

[8] M. Johansson, T. Mattisson, A. Lyngfelt, A. Abad. Fuel, 87 (2008) 988-1001.

[9] L.F. de Diego, M. Ortiz, J. Adánez, F. García-Labiano, A. Abad, P. Gayán. Chem. Eng. J., 144 (2008) 289-298

[10] P. Gayán, L. F. de Diego, F. García-Labiano, J. Adánez, Alberto Abad, C. Dueso. Fuel, 87 (2008) 2641–2650

[11] J. Adánez, L.F. de Diego, F. García-Labiano, P. Gayán, A. Abad and J.M. Palacios. Energy Fuels, 18 (2004) 371-377

[12] L.F. de Diego, F. García-Labiano, J. Adánez, P. Gayán, A. Abad, B.M. Corbella and J.M. Palacios. Fuel, 83 (2004) 1749-1757

Captions for the Figures

Figure 1: Chemical-Looping Reforming.

Figure 2: Schematic diagram of the Chemical-Looping Reforming facility.

Figure 3: Effect of fuel reactor temperature on the gas product concentrations working with the oxygen carrier Ni18-αAl_2O_3. H_2O/CH_4 = 0.3; NiO/CH_4= 1.3.

Figure 4: Effect of fuel reactor temperature on the gas product concentrations working with the oxygen carrier Ni21-γAl_2O_3. H_2O/CH_4 = 0.3; NiO/CH_4= 1.8.

Figure 5: Effect of oxygen carrier-to-fuel ratio on the gas product concentrations with different H_2O/CH_4 molar ratios for the Ni21-γAl_2O_3 oxygen carrier. T = 900ºC

Figure 6: Effect of oxygen carrier-to-fuel ratio on the gas product concentrations with different H_2O/CH_4 molar ratios for the Ni18-αAl_2O_3 oxygen carrier. T = 900ºC

Figure 7: Reactivity in TGA of the oxygen carriers. T_{redu} = 900ºC, T_{oxid} = 950ºC.

Figure 8: Conversions reached by the oxygen carriers in the pilot plant. T = 900ºC, H_2O/CH_4=0.3

Figure 9: Effect of $NiO_{reacted}/CH_4$ molar ratio on the gas product composition for both oxygen carriers. Filled dots: NiO18-αAl_2O_3. Empty dots: NiO21-γAl_2O_3 Lines: thermodynamic equilibrium data. (□, ■, ……): H_2O/CH_4 = 0, (○, ●, -----): H_2O/CH_4 = 0.3, (Δ, ▲, ──): H_2O/CH_4 = 0.5.

Figure 10: Evolution of the pore size distribution of the oxygen carriers during CLR operation. (a) NiO21-γAl_2O_3 , (b) NiO18-αAl_2O_3.

Figure 11: SEM images of the NiO21-γAl_2O_3 oxygen carrier, (a) fresh particles, (b) particles used for 50 hours in the CLR prototype, and EDX analysis for Ni distribution in the cross section of the particle.

Table 1. Physical properties and solid composition of the oxygen carriers

Oxygen carrier	**Density ($g\ cm^{-3}$)**	**Crushing strength (N)**	**BET ($m^2\ g^{-1}$)**	**Porosity (%)**	**XRD**
NiO21-γAl_2O_3 Fresh	1.7	2.6	83.4	50.7	γ-Al_2O_3, $NiAl_2O_4$
NiO21-γAl_2O_3 After 50 h operation	1.9	2.4	29	48.4	γ-Al_2O_3, $NiAl_2O_4$, NiO
NiO18-αAl_2O_3 Fresh	2.4	4.1	7	42.5	α-Al_2O_3, NiO, $NiAl_2O_4$
NiO18-αAl_2O_3 After 50 h operation	2.5	4.0	5.4	40.8	α-Al_2O_3, NiO, $NiAl_2O_4$

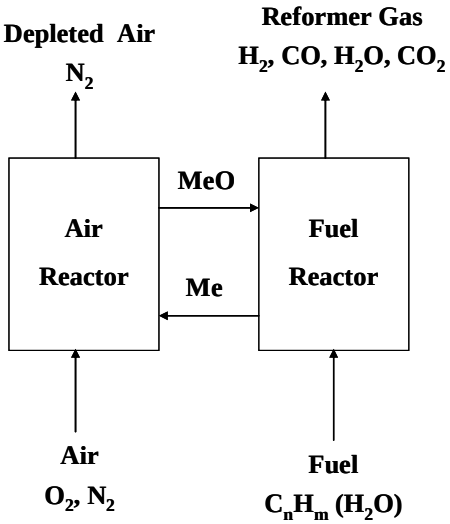

Figure 1: Chemical-Looping Reforming.

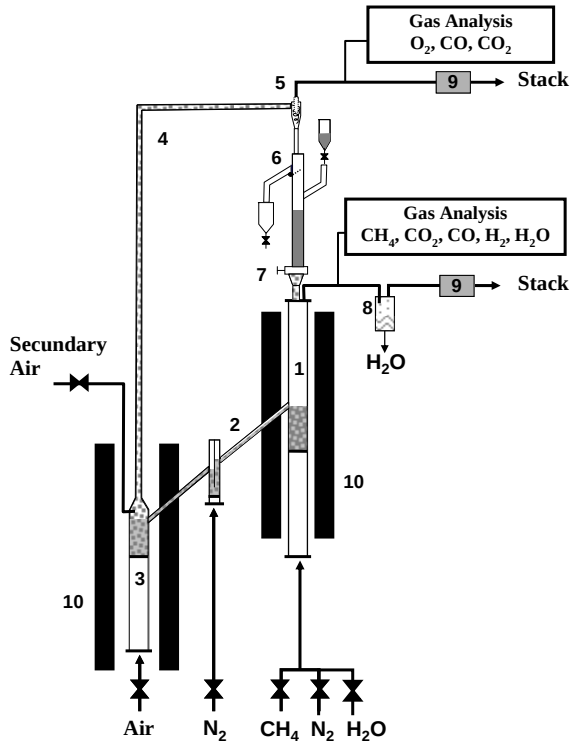

Figure 2: Schematic diagram of the Chemical-Looping Reforming facility.

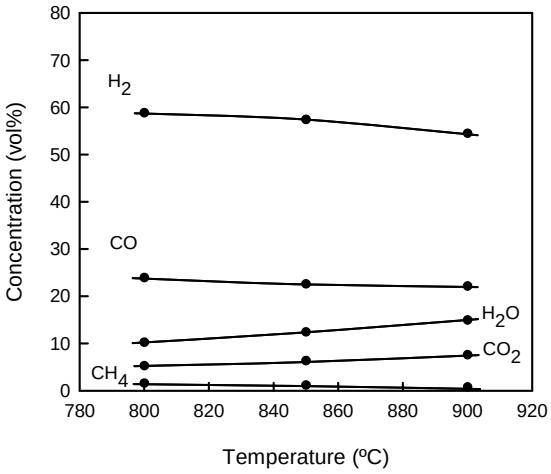

Figure 3: Effect of fuel reactor temperature on the gas product concentrations working with the oxygen carrier Ni18-αAl_2O_3. H_2O/CH_4 = 0.3; NiO/CH_4= 1.3.

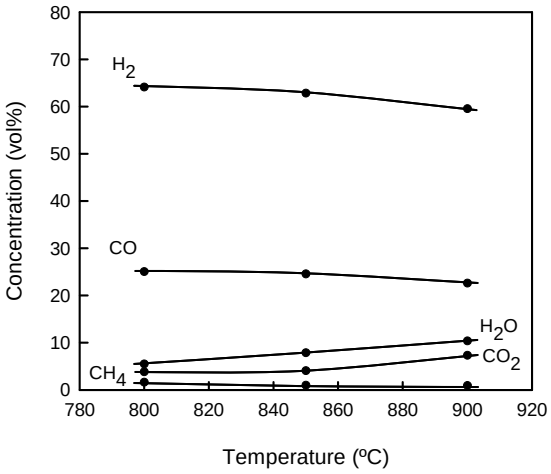

Figure 4: Effect of fuel reactor temperature on the gas product concentrations working with the oxygen carrier Ni21-γAl_2O_3. H_2O/CH_4 = 0.3; NiO/CH_4= 1.8.

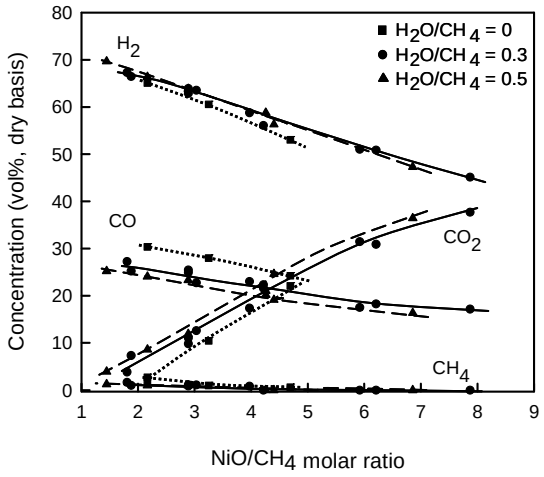

Figure 5: Effect of oxygen carrier-to-fuel ratio on the gas product concentrations with different H_2O/CH_4 molar ratios for the Ni21-γAl_2O_3 oxygen carrier. T = 900ºC.

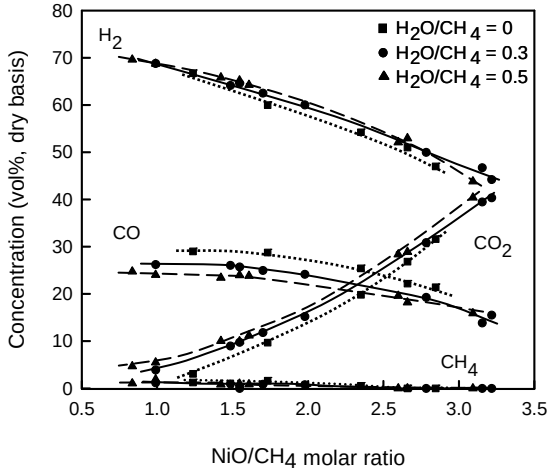

Figure 6: Effect of oxygen carrier-to-fuel ratio on the gas product concentrations with different H_2O/CH_4 molar ratios for the Ni18-αAl_2O_3 oxygen carrier. T = 900ºC.

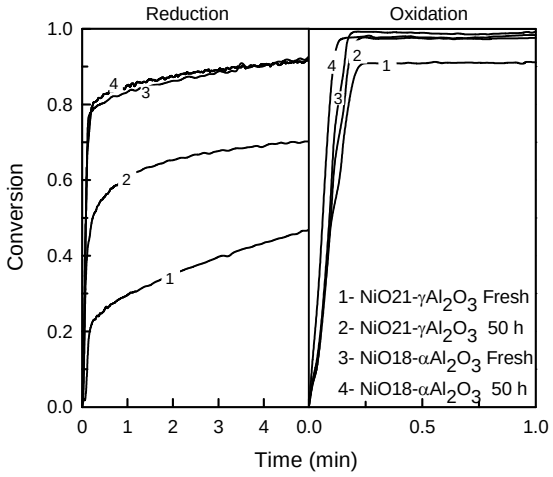

Figure 7: Reactivity in TGA of the oxygen carriers. T_{redu} = 900 ºC, T_{oxid} = 950 ºC.

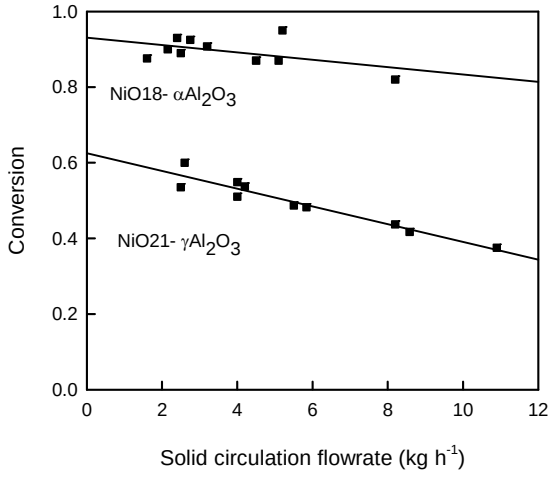

Figure 8: Conversions reached by the oxygen carriers in the pilot plant. T= 900ºC, H_2O/CH_4=0.3

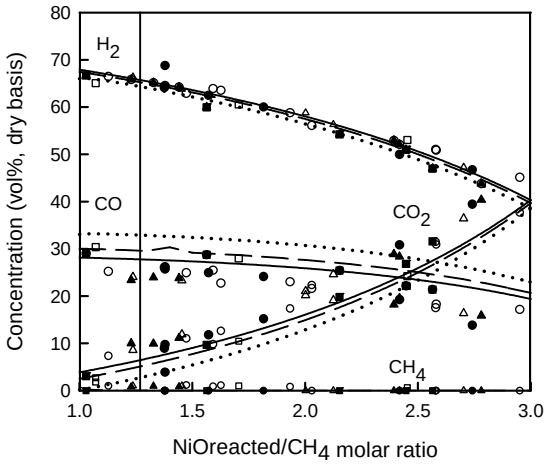

Figure 9: Effect of $NiO_{reacted}/CH_4$ molar ratio on the gas product composition for both oxygen carriers. Filled dots: NiO18-αAl_2O_3. Empty dots: NiO21-γAl_2O_3 Lines: thermodynamic equilibrium data. (□, ■, ·····): $H_2O/CH_4 = 0$, (○, ●, -----): $H_2O/CH_4 = 0.3$, (Δ, ▲, ——): $H_2O/CH_4 = 0.5$.

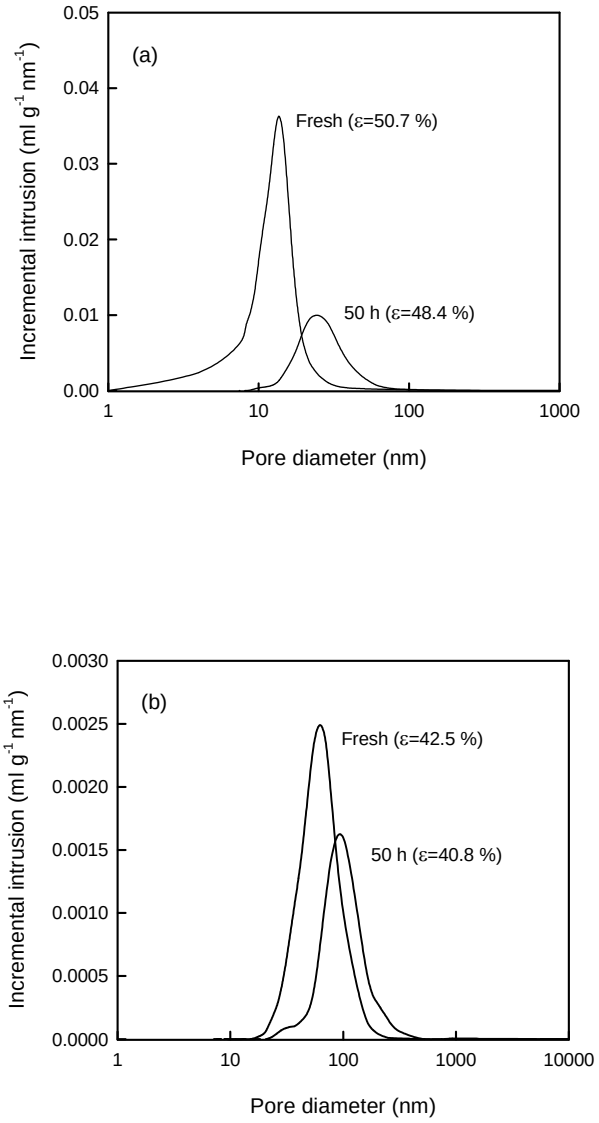

Figure 10: Evolution of the pore size distribution of the oxygen carriers during CLR operation. (a) NiO21-γAl_2O_3 , (b) NiO18-αAl_2O_3.

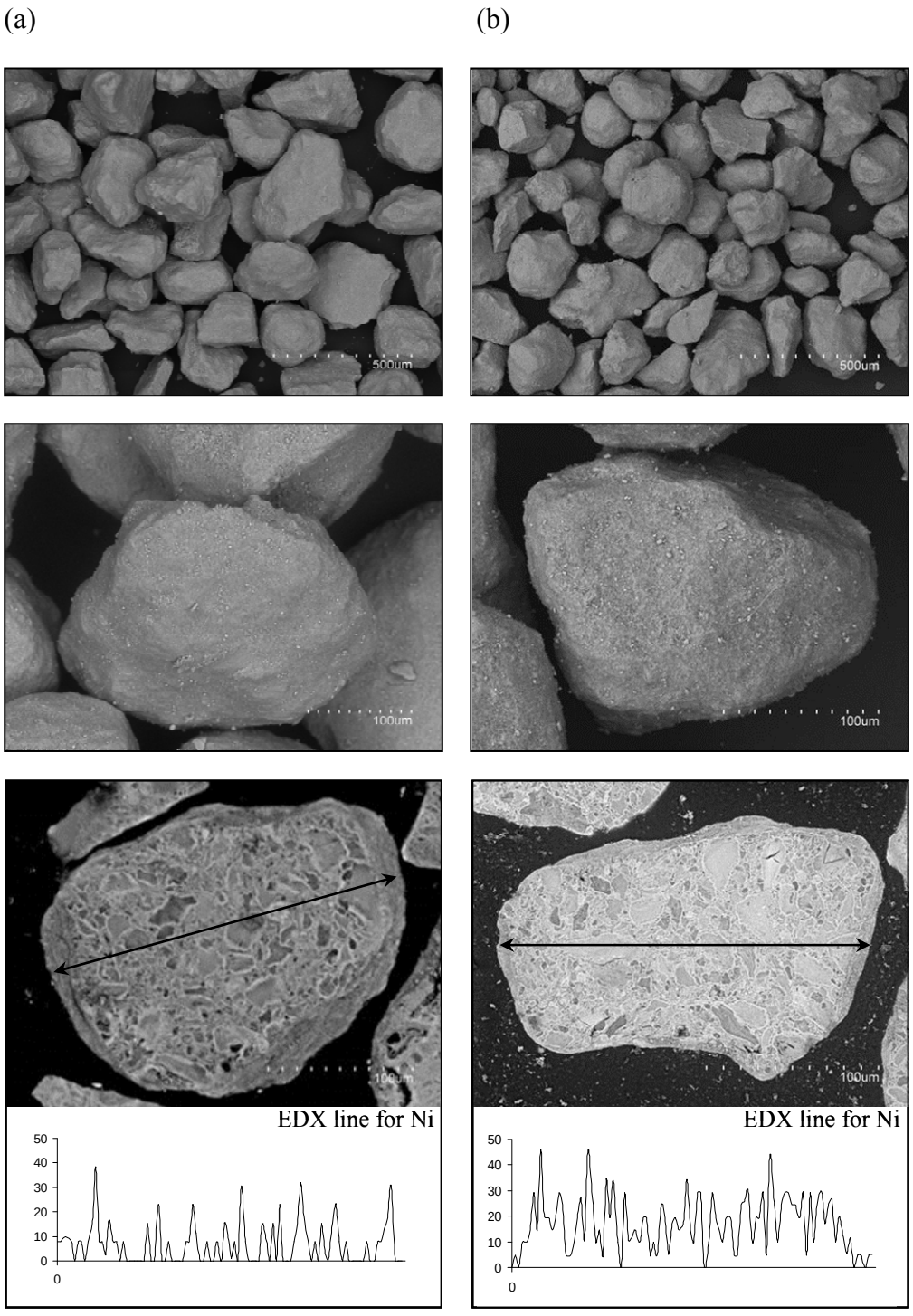

Figure 11: SEM images of the NiO21-γAl_2O_3 oxygen carrier, (a) fresh particles, (b) particles used for 50 hours in the CLR prototype, and EDX analysis for Ni distribution in the cross section of the particle.